Application of Frequency Map Analysis to the BEPC Ⅱ Lattice*

JIAO Yi[1)] ZHOU De-Min WANG Jiu-Qing QIN Qing XU Gang FANG Shou-Xian

(Institute of High Energy Physics, CAS, Beijing 100049, China)

Abstract The frequency map analysis (FMA) method is systematically applied to the lattice of the BEPC Ⅱ storage ring for the first time in this paper. We compute characteristic parameters of the lattice with the Accelerator Toolbox (AT) code, in which the FMA method is imbedded, and compare the results with those of MAD and SAD codes. The lattices of the BEPC Ⅱ collision and injection modes are analyzed and optimized using FMA with the RF cavity and radiation on. Both on- and off-momentum frequency maps are studied to have a complete picture of dynamics. The synchro-betatron resonance is found to have large effect on the beam dynamics.

Key words accelerator toolbox, frequency map analysis, BEPC Ⅱ, synchro-betatron resonance

1 Introduction

BEPC Ⅱ is the upgrade project of the Beijing Electron Positron Collider (BEPC) being built at IHEP. To enhance its luminosity, a double-ring design is adopted to house the micro-β scheme and multi-bunch collision. For the colliding beams the design luminosity is $1\times10^{33}\mathrm{cm}^{-2}\mathrm{s}^{-1}$ optimized at beam energy 1.89GeV, which is about two orders higher than that of the BEPC[1]. The beam-beam simulations with Cai's code[2] and Zhang's code[3] show that 0.51/0.58 is the best working point region for the BEPC Ⅱ to reach the design luminosity. However, the working point is so much close to the half integer resonance that the nonlinearities could be large and the consequent optimization becomes rather difficult. In addition, some possible measures to improve the luminosity include reducing the vertical beta function at IP and decreasing the momentum compaction factor correspondingly, which will also enhance the difficulty of finding a good beam dynamics.

Frequency map analysis (FMA) is a very useful tool to study the single particle dynamics by constructing a one-to-one relationship between the space of initial conditions (x, y, $x'=y'=0$) and the tune space (Q_x, Q_y)[4]. With this method, we can obtain the dynamic aperture (DA) and the corresponding frequency map (FM) at the same time, and study the effects and features of only one resonance out of others. This method has been first applied to the ALS at LBNL[5], and then widely used on many other machines (NSLS, SPEAR3, SOLEIL, ESRF, SSRF, etc.)[6—10]. It is the first time to introduce the FMA to analyze the lattice of the BEPC Ⅱ storage ring. The DAs and FMs for the lattices of the collision and injection modes are computed with the symplectic tracking code AT, aiming to understand the limit of beam dynamics and make further optimization.

The paper is organized as follows. In Sec. 2, we track the collision mode at the working point of (6.51, 5.58) with the codes of AT, MAD and SAD, and then make a comparison of the results. The FMA results of BEPC Ⅱ lattices, i.e., the frequency map, the tune shifts with amplitude and the single resonance struc-

Received 20 September 2006, Revised 20 October 2006

* Supported by National Natural Science Foundation of China (10375076)

1) E-mail: jiaoyi@ihep.ac.cn

ture, are presented in Sec. 3. Further optimizations of the lattices based on the FMA analysis results are also described in Sec. 3. We summarize and conclude our work in Sec. 4.

2 Codes crosscheck

2.1 Linear lattice

The BEPCⅡ lattice loses the 4-fold symmetry of the BEPC, due to the double-ring geometric structure. A pair of defocusing superconducting quadrupoles is used to squeeze the vertical beta function at the IP. The dispersion functions are free at the IP, the RF region (outer rings) and the injection points. The beta functions are required to be less than 15m at the RF cavities in both vertical and horizontal planes and bigger than 20m at the injection point in horizontal plane to save the kicker strength.

A recently designed collision mode lattice[11], whose main parameters and optical functions are given in Table 1 and Fig. 1 respectively, is used for comparing the different codes.

Table 1. Main parameters of the BEPCⅡ collision mode.

beam energy E/GeV	1.89
circumference C/m	237.53
RF voltage $V_{\rm rf}$/MV	1.5
betatron/synchrotron tune $Q_x/Q_y/Q_{\rm s}$	6.51/5.58/0.034
natural chromaticity Q'_x/Q'_y	−10.7/−21.0
horizontal natural emittance ε_x/(nm·rad)	141
β function at IP(β^*_x/β^*_y)/m	1/0.015

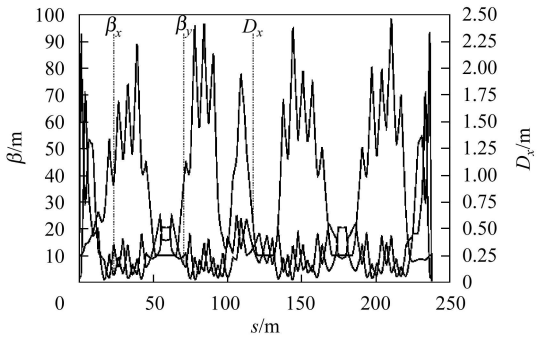

Fig. 1. Optical functions for the BEPCⅡ collision mode, starting at the IP.

2.2 Code comparison

The accelerator design codes usually used in IHEP are MAD[12] and SAD[13], between which the former is mainly used to design the linear lattice and the latter to simulate the DA of the BEPCⅡ storage ring. Since the FMA method is imbedded in the AT[14], it is necessary to check the usability and validity of AT before we apply FMA to the BEPCⅡ lattice.

The linear parameters, such as the working point, the beta function and the chromaticity, are compared between the AT and MAD codes. The AT gives the same working point and beta functions as the MAD code. However, the calculated chromaticity is different by about 0.5 in x and about 0.05 in y, which is possibly due to the fact that AT uses two exact orbit of $\Delta p/p$ (momentum deviation) apart to compute the chromaticity while MAD approximates the off-momentum orbit with terms up to $(\Delta p/p)^2$ [1)]. Anyway, to reduce the difference, we add a term of momentum dependence in the AT dipole fringe field code and the difference becomes smaller than 0.1 in both x and y. Tune variations with $\Delta p/p$ calculated by these two codes reach a good agreement, as shown in Fig. 2.

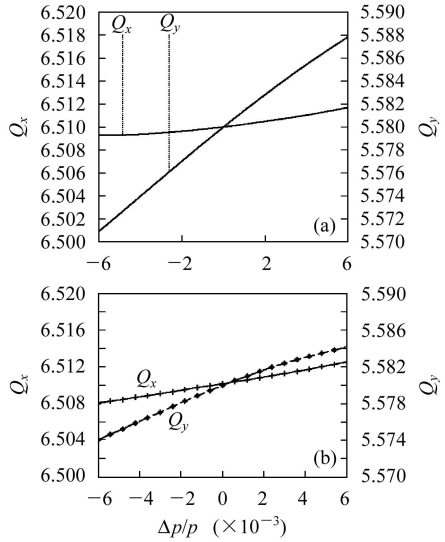

Fig. 2. Tune variations with $\Delta p/p$ for the BEPCⅡ collision mode given by MAD (a) and AT (b).

The DAs are computed with AT and SAD, respectively. Both the simulations are performed for single particles over 2000 turns, taking account of no magnetic field errors but the effects of the RF cavity and synchrotron radiation. The vertical emittance is taken as half of the horizontal natural emittance. The

1) Terebilo A. private communication, 2006.

limit of the longitudinal momentum acceptance due to the RF cavity is ± 0.006, i.e., about $12\sigma_e$. Comparisons are given in Fig. 3 and Table 2. It shows that the DA obtained with SAD is larger than that with AT, especially in the direction of x and y axes. However, if looking carefully, we will find that the sharp protrusions near the axes contribute to the bigger value in the DA obtained with SAD, but will not lead to a better beam dynamics. Therefore the on-momentum DA has to be reduced to $30\sigma_x$ in x and $28\sigma_y$ in y and it is similar for the off-momentum case. Furthermore, the DAs in 45° are almost the same in the two figures. Similar crosschecks of AT and SAD are made based on other BEPC Ⅱ lattices, showing that the DAs obtained with these two codes are always different in the direction of the x and y axes. But the DAs in 45°, which are thought to reflect the actual or effective DA size in a higher degree, agree well between the results of AT and SAD. Therefore it is reasonable to reach the conclusion that the nonlinear tracking from AT is more or less in accord with SAD.

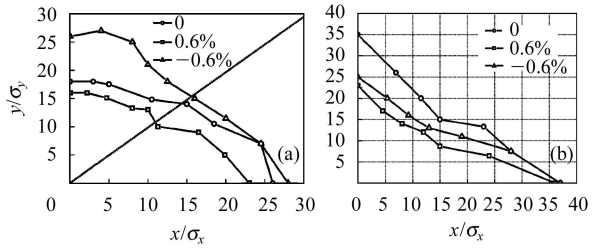

Fig. 3. DAs given by AT (a) and SAD (b), tracking 1000 turns, the unit is σ_x and σ_y. The dashed lines in (a) and (b) indicate the direction of "45°".

It should be mentioned that the tracking performed on the BEPC Ⅱ lattice includes longitudinal oscillation, but only the transverse dynamics was taken into account when FMA was applied to most of the light sources.

Table 2. Comparisons of the AT and SAD tracking results.

code	$\Delta p/p$	$x_{\max}$	$y_{\max}$	$x(45°)$	$y(45°)$
AT	−0.6%	$23\sigma_x$	$16\sigma_y$	$11\sigma_x$	$10\sigma_y$
	0	$28\sigma_x$	$26\sigma_y$	$16\sigma_x$	$15\sigma_y$
	+0.6%	$26\sigma_x$	$18\sigma_y$	$15\sigma_x$	$14\sigma_y$
SAD	−0.6%	$37\sigma_x$	$25\sigma_y$	$13\sigma_x$	$13\sigma_y$
	0	$37\sigma_x$	$35\sigma_y$	$15\sigma_x$	$15\sigma_y$
	+0.6%	$36\sigma_x$	$23\sigma_y$	$12\sigma_x$	$12\sigma_y$

3 FMA on the BEPC Ⅱ lattice

3.1 BEPC Ⅱ collision mode

A. Dynamics of the BEPC Ⅱ collision mode

For the collision mode with the working point of (6.51, 5.58) which has been described in Sec. 2, a problem remains. The nonlinear optimization of the lattice, i.e., 4 families of sextupoles being matched with MAD, is not perfect. As shown in Fig. 4, the average off-momentum DAs with errors (20 random seeds) are just bigger than the required aperture for collision, say $10\sigma_x \times 10\sigma_y$, labeled as the solid square, but smaller than the requirements for injection, i.e., $13.5\sigma_x \times 10\sigma_y$, the dashed square. The minimum DAs with errors (among 20 random seeds) for different momentum deviations are even smaller (for more details, refer to Ref. [11]).

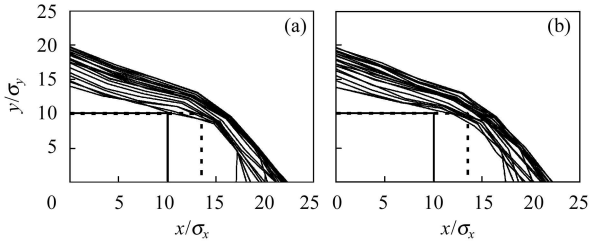

Fig. 4. The average DAs with $\Delta p/p \in (-10\sigma_e, 10\sigma_e)$ from SAD ((a) with only multipolar magnetic errors; (b) with magnetic errors including misalignments and closed orbit correction)[11].

The lattice is put into tracking for 2000 turns, together with the post-processing. The details of the on- and off-momentum DAs (without any errors) are scrutinized using FMA , aiming to find out some factors limiting the beam dynamics.

The DAs and FMs are given in Fig. 5 and the tune shifts with amplitude are plotted in Fig. 6. There is no obvious evidence to support that the DAs are limited by any resonance (if there is any evidence at all, one possible resonance is $2Q_x - Q_s = 13$). Corresponding to the great disparity between the on- and off-momentum DAs, the on- and off-momentum FMs are also very different. That is, the off- momentum FMs are not folded like the on-momentum case and the tune footprints cover the range $Q_x \in (6.514, 6.516)$ with a higher diffusion rate or even particle loss.

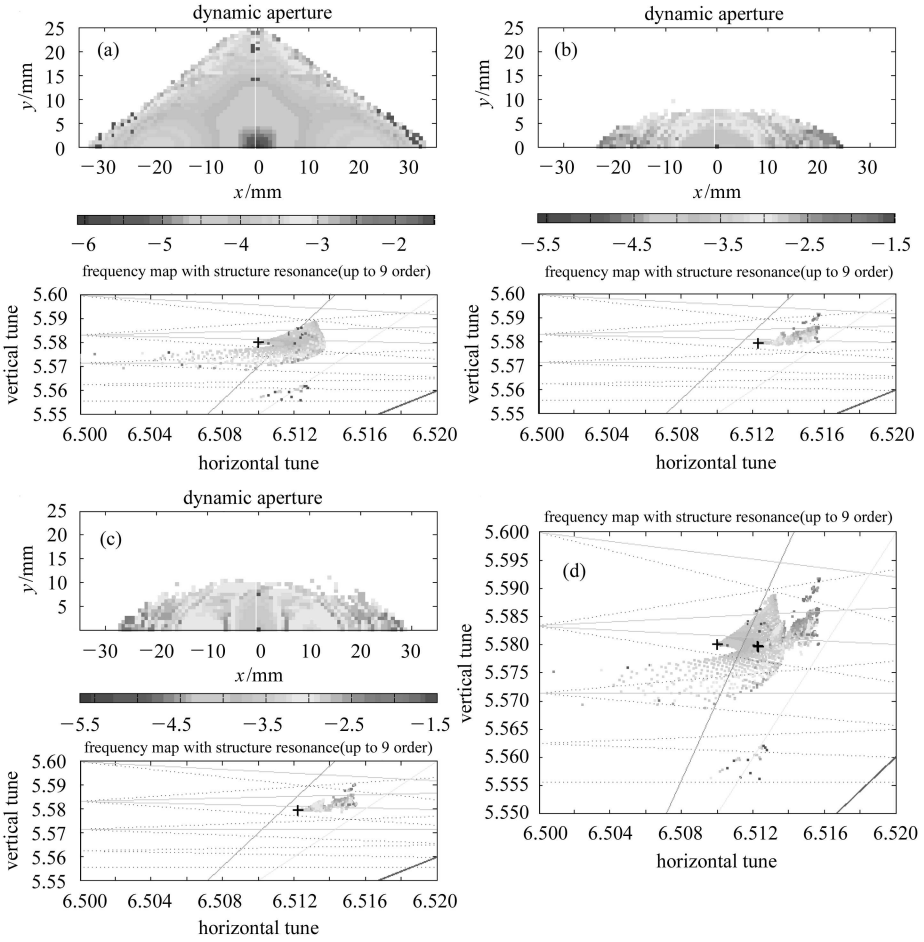

Fig. 5. The frequency maps with $\Delta p/p$=0 (a), −0.006 (b) and 0.006 (c), respectively. (d) shows the tune footprints with three cases together. The color scale corresponds to the orbit diffusion from regular to chaotic motion.

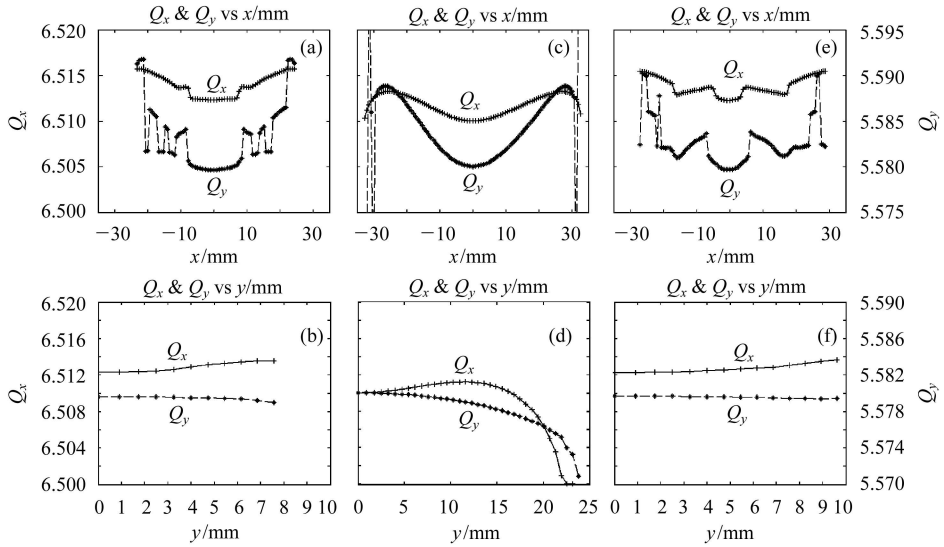

Fig. 6. Tune shifts vs. amplitude of the collision mode for $\Delta p/p$=−0.006 ((a) & (b)), 0 ((c) & (d)) and 0.006 ((e) & (f)), respectively. In each case the fixed coordinate x or y is set to 1μm.

It shows that the single particle dynamics is sensitive to $\Delta p/p$. For particles with $\Delta p/p = 0$, the arrangement of the sextupoles compensates the nonlinear driving terms well. But for particles with $\Delta p/p \neq 0$, the nonlinearity seems to be very strong. Indeed, this can be explained with the the-

ory of super-periodic structural resonances analysis (SSRA)[10, 15]. According to SSRA, the half integer resonance $2Q_x$=13 is a second order super-periodic structural resonance stopband with strong nonlinearity for the BEPC Ⅱ lattice, which has only one superperiod in each ring. When the working point gets closer to the stopband, the chromaticity correction and nonlinear optimization become more difficult.

B. Further optimization of the collision mode

18 groups instead of 4 groups of sextupoles are used to optimize the nonlinear lattice with the SAD chromaticity correction. The variations of beta function and its derivative with $\Delta p/p$ are strictly controlled to reduce the lattice sensitivity to $\Delta p/p$. Consequently, the on- and off-momentum DAs and FMs become quite similar. However, the DAs with different momentum deviations become smaller as a whole than that before optimization.

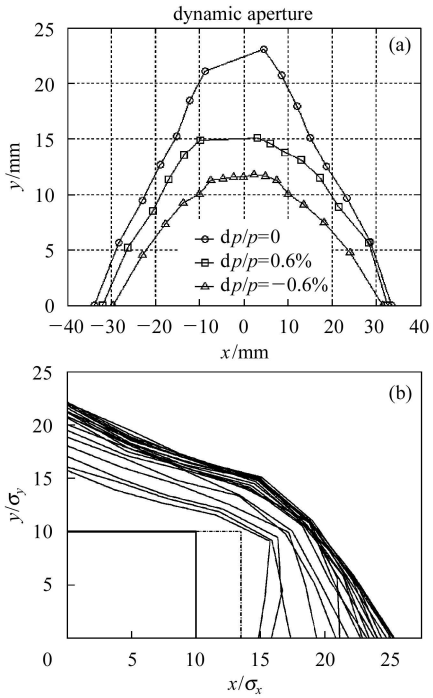

Fig. 7. The optimized DAs. (a) AT result without errors; (b) SAD result with errors and $\Delta p/p \in (-10\sigma_e, 10\sigma_e)$.

Another big effort is made to find a set of sextupoles with smaller anharmonicities dQ_x/dx^2, dQ_x/dy^2 and dQ_y/dy^2. We use 8 groups of sextupoles for nonlinear optimization and change the (dQ_x/dx^2, dQ_x/dy^2, dQ_y/dy^2) from (73, 77, 208) to (70, 68, 198). Although the disparity between the on- and off-momentum DAs and FMs still exists, all the DAs without errors are slightly larger than that before optimization, and the average DAs with errors (20 random seeds) satisfy the requirement for beam injection, shown in Fig. 7.

3.2 BEPC Ⅱ injection mode

A. Dynamics of the BEPC Ⅱ injection mode

The injection mode relaxes the constraints on the low vertical beta function at the IP and the working point close to half integer resonances, but calls for larger DA and better beam dynamics. We choose the working point as (6.58, 5.62), which is located in a relatively clean area in tune space. The main parameters of this mode are given in Table 3.

Table 3. Main parameters of the BEPC Ⅱ injection mode.

beam energy E/GeV	1.89
circumference C/m	237.53
RF voltage V_{rf}/MV	1.5
betatron/synchrotron tune $\nu_x/\nu_y/\nu_s$	6.58/5.62/0.034
natural chromaticity ν'_x/ν'_y	−10.5/−12.1
horizontal natural emittance ε_x/(nm·rad)	135
β function at IP (β^*_x/β^*_y)/m	2.8/0.04

The tracking is performed over 2000 turns without errors, with the last 1000 turns being devoted to the diffusion computation. The on- and off-momentum beam dynamics is similar, thus only the on-momentum case is analyzed. The results are given in Fig. 8 and Fig. 9. The DA is large, namely, $[-30, 45]_{y=0}\times[0, 42]_{x=0}$mm. From the one-to-one correspondence between the DA and FM, we find that the horizontal DA is limited by the transverse coupling resonance $Q_x - Q_y$=1. Furthermore, we find the synchro-betatron resonance $2Q_x+3Q_y+Q_s$=30 is located at the border of the DA, i.e., it limits the stability area. On the contrary, the corresponding pure transverse resonance $2Q_x+3Q_y$=30 has much less effect on the beam dynamics [see Fig. 10(a)]. It shows that when the longitudinal oscillation is considered, the single particle beam dynamics may have a lot of changes and need to be re-analyzed. The synchro-betatron resonance may affect the beam dynamics seriously and enough attention should be paid to it.

B. Further optimization of the injection mode

If we keep the tune footprints away from the reso-

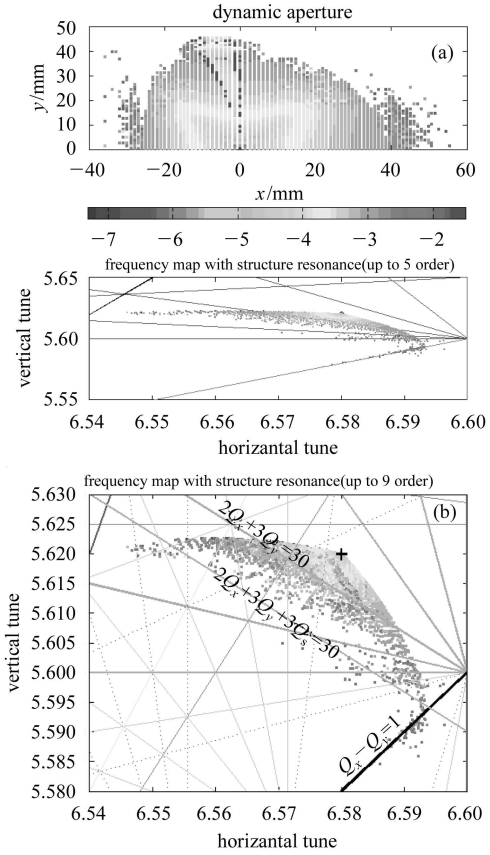

Fig. 8. Dynamic aperture and frequency map of the injection mode lattice with $\Delta p/p$=0 (a); frequency maps with $\Delta p/p$=0, ±0.006 together (b).

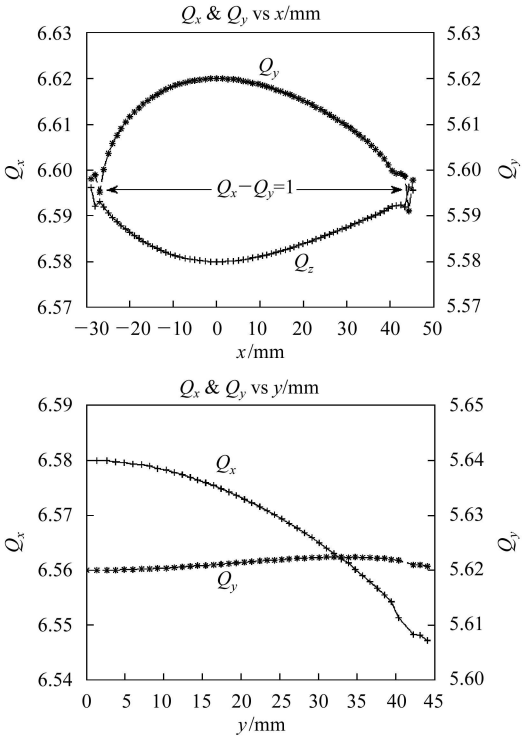

Fig. 9. Tune shifts vs. amplitude of the injection mode with $\Delta p/p$=0.

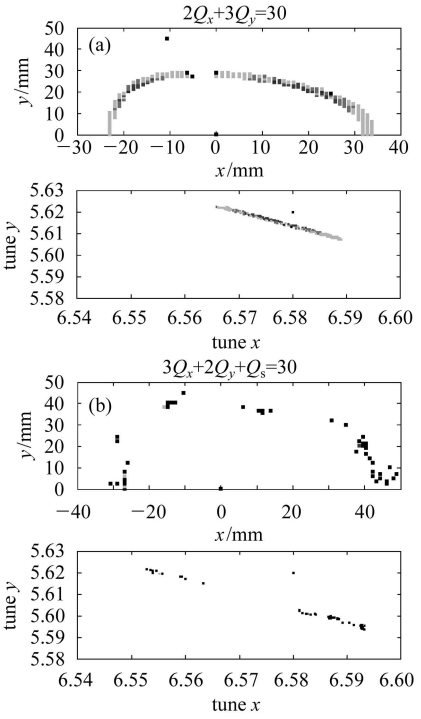

Fig. 10. Locations of the resonances $2Q_x+3Q_y$=30 (a) and $2Q_x+3Q_y+Q_s$=30 (b) in tune space and space of initial conditions.

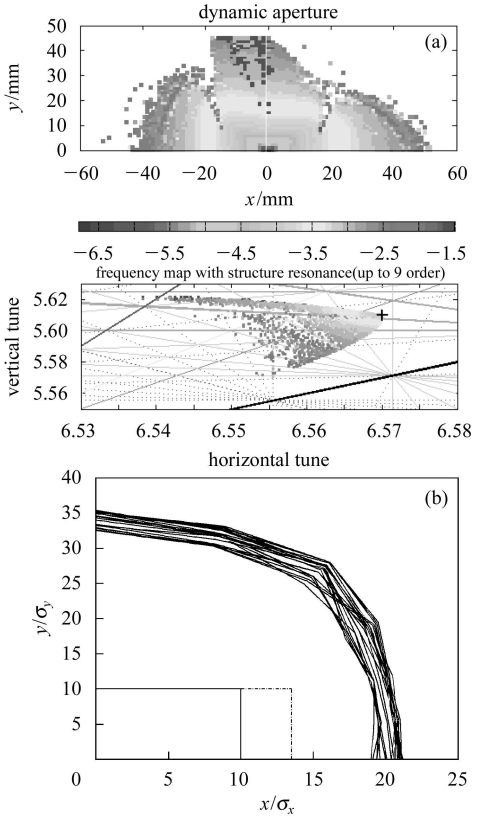

Fig. 11. The DA and FM without errors given by AT (a); the average DAs including errors with $\Delta p/p \in(-10\sigma_e, 10\sigma_e)$ given by SAD (b).

nance $2Q_x+3Q_y+Q_s=30$ and $Q_x-Q_y=1$, the limit of the dynamics will vanish and the DA will be larger. Optimizations based on this idea are performed. The working point is moved to (6.57, 5.61), and the amplitude tune shift slope at origin is reduced from $(\mathrm{d}Q_x/\mathrm{d}x^2)_{x=0}=760$ to 133. As shown in Fig. 11, the optimized DA (without errors) increases to be $[-40, 50]_{y=0}\times[0, 45]_{x=0}$mm. The DA (with error) obtained with SAD is much bigger than the requirements of the injection mode, which confirms our optimization.

4 Conclusion

The analyses and further optimizations of the BEPCⅡ collision and injection modes with FMA are described in this paper. FMA turns out to be a good and effective tool to look into the beam dynamics and the resonance structure in a global way, thus enabling us to avoid dangerous areas in tune space and to further improve the beam dynamics.

The RF cavity and synchrotron radiation are turned on during the tracking, that is, the longitudinal oscillation is taken into account. The synchro-betatron resonances may be exited and have large effect on the dynamics of the BEPCⅡ lattices. In the case of the injection mode with the working point of (6.58, 5.62), such a resonance is responsible for the limit of the DA. When we move the working point away from the resonance, the DA significantly increases.

The horizontal working point of the collision mode is very close to the half integer resonance, which is expected to be a second order super-periodic structural resonance with strong nonlinearity. The chromaticity correction of sextupoles does not have enough effective action range of momentum deviations, leading to a great disparity between the on- and off-momentum beam dynamics and the difficulty of nonlinear optimization.

References

1 IHEP-BEPCⅡ-SB-03-3, 2003 (in Chinese)
(北京正负电子对撞机重大改造工程BEPCⅡ初步设计——储存环, 2003)
2 XU G. Machine Physics Issues and Preparation for Commissioning, IHEP-URAP-Note/2005-06. 2005
3 ZHANG Y. Study of Beam-Beam Effects in e^+e^- Storage Ring Collider. Ph. D Thesis, 2005 (in Chinese)
(张源. 正负电子储存环对撞机中的束束效应研究. 博士论文, 2005)
4 Nadolski L, Laskar J. Phys. Rev. ST Accel. Beams, 2003, **6**: 114801
5 Steier C et al. EPAC 2002, 1077; Robin D et al. Phys. Rev. Lett., 2000, **85**: 558
6 Belgroune M et al. EPAC 2002. 1229
7 Papaphilippou Y et al. PAC 2003. 3189; Papaphilippou Y et al. EPAC 2003. 2050
8 Papaphilippou Y. PAC 2001. 462
9 Terebilo A et al. PAC 1998. 1457
10 JIAO Y et al. NIM, 2006, **A566**: 270
11 QIN Q. Internal Report, IHEP-AC-AP-Note/2006-01, 2006
12 MAD Code Homepage, http:// mad.web.cern.ch/mad/
13 SAD Code Homepage, http://acc-physics.kek.jp/SAD/sad.html
14 AT Code Homepage, http://www-ssrl.slac.stanford.edu/at/welcome.html
15 FANG S X, QIN Q. HEP & NP, 2006, **30**(9): 880 (in Chinese)
(方守贤, 秦庆. 高能物理与核物理, 2006, **30**(9): 880)

FMA在BEPCⅡ上的应用*

焦毅[1)] 周德民 王九庆 秦庆 徐刚 方守贤

(中国科学院高能物理研究所 北京 100049)

摘要 介绍了基于AT的FMA方法在BEPCⅡ上首次较系统的应用. 将AT分析结果与MAD和SAD程序比较, 吻合较好. 考虑高频腔和辐射阻尼效应, 利用FMA分别对BEPCⅡ对撞模式和注入模式进行分析, 揭示了相应的单粒子动力学, 为进一步优化提供指导和依据. 结果显示纵向横向耦合共振可能会对粒子动力学产生较大影响.

关键词 AT FMA BEPCⅡ 纵向横向耦合共振

2006 – 09 – 20 收稿, 2006 – 10 – 20 收修改稿

* 国家自然科学基金(10375076)资助

1) E-mail: jiaoyi@ihep.ac.cn